

This suggests that the primary role for cIAP-1 and cIAP-2 is to block caspase 8 activation. It also verifies a previous proposal that cIAPs act downstream of NF- κ B during its cell survival pathway (25, 26). NF- κ B signaling is insufficient to block the onset of apoptosis in the presence of Smac or compound 3. The ability of compound 3 to potentiate apoptosis in TNF α -treated cells, despite NF- κ B activation, suggests a strategy for treating inflammatory disease such as rheumatoid arthritis (RA). TNF α functions in RA by inducing secretion of matrix-degrading proteases and multiple inflammatory cytokines and chemokines and increased expression of class I major histocompatibility molecules by synovial fibroblasts (leading to cartilage and bone erosion) and synovial neoangiogenesis (27). Moreover, it stimulates adhesion molecules on the surface of vascular endothelial cells to recruit circulating leukocytes to the endothelium and activates multinucleated osteoclasts to form a seal around bone, where they cause erosion by acidic secretions and protease activity (28). If the original TNF α signal terminated in cell death, it is possible that these downstream events would be avoided.

References and Notes

1. N. A. Thornberry, Y. Lazebnik, *Science* **281**, 1312 (1998).
2. Q. L. Deveraux, J. C. Reed, *Genes Dev.* **13**, 239 (1999).
3. X. Wang, *Genes Dev.* **15**, 2922 (2001).
4. J. Chai *et al.*, *Nature* **406**, 855 (2000).
5. A. G. Uren, M. Pakusch, C. J. Hawkins, K. L. Puls, D. L. Vaux, *Proc. Natl. Acad. Sci. U.S.A.* **93**, 4974 (1996).
6. M. Rothe, M. G. Pan, W. J. Henzel, T. M. Ayres, D. V. Goeddel, *Cell* **83**, 1243 (1995).
7. I. Imoto *et al.*, *Cancer Res.* **61**, 6629 (2001).
8. T. Hasegawa *et al.*, *Blood* **101**, 1164 (2003).
9. M. Krajewska *et al.*, *Clin. Cancer Res.* **9**, 4914 (2003).
10. C. Du, M. Fang, Y. Li, L. Li, X. Wang, *Cell* **102**, 33 (2000).
11. A. M. Verhagen *et al.*, *Cell* **102**, 43 (2000).
12. Single-letter abbreviations for the amino acid residues are as follows: A, Ala; E, Glu; F, Phe; I, Ile; K, Lys; P, Pro; Q, Gln; and V, Val.
13. G. Wu *et al.*, *Nature* **408**, 1008 (2000).
14. Z. Liu *et al.*, *Nature* **408**, 1004 (2000).
15. S. Fulda, W. Wick, M. Weller, K. M. Debatin, *Nat. Med.* **8**, 808 (2002).
16. O. E. Pardo *et al.*, *Mol. Cell. Biol.* **23**, 7600 (2003).
17. L. Yang *et al.*, *Cancer Res.* **63**, 831 (2003).
18. C. R. Arnt, M. V. Chiorean, M. P. Heldebrandt, G. J. Gores, S. H. Kaufmann, *J. Biol. Chem.* **277**, 44236 (2002).
19. This nomenclature refers to the AVPF prototype where the N-terminal L-alanine is position 1 and L-phenylalanine is position 4. Ten surrogates for a proline-phenylalanine dipeptide and 18 variable amino acid residues at position two were combined for a total of 180 compounds.
20. The conversion of 2 to 3 shown in Fig. 1A is an optimized version (29) of an oxidation first observed as a minor competing pathway during Cu^I-catalyzed cycloadditions of 2 to alkyl azides.
21. M. Mammen, S.-K. Choi, G. M. Whitesides, *Angew. Chem. Int. Ed. Engl.* **37**, 2754 (1998).
22. Y. Huang, R. L. Rich, D. G. Myszk, H. Wu, *J. Biol. Chem.* **278**, 49517 (2003).
23. Under conditions identical to those used in Fig. 1F, neither Smac nor compound 3 block the interaction of XIAP with activated caspases 3. However, both relieve XIAP suppression of caspase 3 activity (fig. S5).

24. Y. Deng, X. Ren, L. Yang, Y. Lin, X. Wu, *Cell* **115**, 61 (2003).
25. C. Y. Wang, M. W. Mayo, R. G. Korneluk, D. V. Goeddel, A. S. Baldwin Jr., *Science* **281**, 1680 (1998).
26. Z. L. Chu *et al.*, *Proc. Natl. Acad. Sci. U.S.A.* **94**, 10057 (1997).
27. D. A. Fox, *Arch. Intern. Med.* **160**, 437 (2000).
28. J. Lam *et al.*, *J. Clin. Invest.* **106**, 1481 (2000).
29. R. Berscheid, F. Vögtle, *Synthesis* **1992**, 58 (1992).
30. We thank O. Guryev for invaluable technical assistance, J. Chen for helpful discussions, N. Williams for preliminary toxicological data, and M. S. Brown and S. L. McKnight for helpful suggestions. Funding provided by a program project grant from the National Cancer

Institute (PO1 CA95471). J.K.D. and P.G.H. are fellows of the Alfred P. Sloan Foundation. P.G.H. acknowledges unrestricted research awards from Eli Lilly, Pfizer, and AstraZeneca. Molecular interaction data have been deposited in the Biomolecular Interaction Network Database with accession codes 150999 to 151001.

Supporting Online Material

www.sciencemag.org/cgi/content/full/305/5689/1471/DC1

Figs. S1 to S6

23 March 2004; accepted 15 June 2004

The Emergence of Competition Between Model Protocells

Irene A. Chen,^{1,2} Richard W. Roberts,³ Jack W. Szostak^{1*}

The transition from independent molecular entities to cellular structures with integrated behaviors was a crucial aspect of the origin of life. We show that simple physical principles can mediate a coordinated interaction between genome and compartment boundary, independent of any genomic functions beyond self-replication. RNA, encapsulated in fatty acid vesicles, exerts an osmotic pressure on the vesicle membrane that drives the uptake of additional membrane components, leading to membrane growth at the expense of relaxed vesicles, which shrink. Thus, more efficient RNA replication could cause faster cell growth, leading to the emergence of Darwinian evolution at the cellular level.

A simple model of a primitive cell involves a self-replicating genome, such as an RNA polymerase ribozyme (a “replicase”), and an encapsulating membrane that can grow and divide (1) (supporting online text). Genomic influence over vesicle growth has been assumed to require a second RNA function, such as a ribozyme that would synthesize membrane components (2). Although such molecules presumably evolved at some point, we wondered whether the transition to a unified cell might have been facilitated by simpler physical mechanisms for coupling genomic properties and membrane behavior.

We sought to detect the emergence of an adaptive cellular-level trait based on the physical properties of a model prebiotic vesicle system containing encapsulated nucleic acids. Counterions associated with RNA encapsulated by a semipermeable membrane exert osmotic pressure on the membrane, which is counterbalanced by membrane tension. RNA replication would convert freely diffusing nucleic acid monomers into large impermeable macromolecules, increasing the concentration of trapped counterions. The re-

sulting increase in osmotic pressure and membrane tension would create a driving force for an increase in membrane area, thereby coupling RNA replication to membrane growth (supporting online text).

We tested whether fatty acid vesicles (3–5) (supporting online text) osmotically stressed by encapsulated contents would increase in membrane area at the expense of unstressed vesicles. An initial concern was that fatty acid membranes might be too structurally weak to maintain a substantial osmotic gradient. We therefore determined the maximum sustainable membrane tension of oleate (C18:1) vesicles under osmotic stress. Oleate vesicles (100-nm diameter) encapsulating 1 M sucrose were diluted into hypotonic buffers (6). Applied gradients ≥ 0.7 M caused transient membrane rupture and release of solutes, detectable by size-exclusion chromatography, followed by membrane resealing at a maximal sustainable membrane tension (τ^*_{oleate}). After accounting for vesicle swelling from the extruded nonspherical shape to a spherical shape (7, 8) and the partial loss of encapsulated solutes, we estimate that τ^*_{oleate} is 10 dyn/cm, or 4 atm. A similar experiment with 100 nm POPC (1-palmitoyl-2-oleoyl-*sn*-glycero-3-phosphocholine) vesicles showed that τ^*_{POPC} is 25 dyn/cm (supporting online text). These measurements fall within the range previously reported for phospholipid membranes (3 to 40 dyn/cm) (9–11). Thus, fatty acids, though chemically simple, can indeed form surprisingly strong membranes under osmotic stress.

¹Department of Genetics, Harvard Medical School, and Howard Hughes Medical Institute, Department of Molecular Biology, Massachusetts General Hospital, Boston, MA 02114, USA. ²Program in Biophysics, Harvard University, Cambridge, MA 02138, USA. ³Division of Chemistry and Chemical Engineering, California Institute of Technology, Pasadena, CA 91125, USA.

*To whom correspondence may be addressed. E-mail: szostak@molbio.mgh.harvard.edu

We then performed competition experiments between swollen and isotonic vesicles. Low-osmolarity (isotonic) oleate vesicles were prepared in buffer without sucrose. High-osmolarity (swollen) vesicles were prepared by encapsulating sufficient osmolyte (e.g., 1 M sucrose) to generate the maximal sustainable membrane tension upon dilution into buffer. The two vesicle preparations were mixed in a stopped-flow device, and membrane surface areas of the swollen and isotonic vesicles were monitored in separate experiments using a fluorescence resonance energy transfer (FRET)-based assay (6). We observed that the membrane area of swollen oleate vesicles increased and the membrane area of isotonic vesicles decreased in parallel by $\sim 25\%$ when mixed in a 1:1 ratio (Fig. 1, A to D), following first-order kinetics ($k_{\text{oleate}} \sim 0.1 \text{ s}^{-1}$). Vesicle fusion, which would result in FRET decreases for both vesicle populations, does not explain the observed changes. No pronounced changes in FRET were seen upon mixing vesicles of equal osmolarity or mixing vesicles with buffer alone. Similar experiments with POPC vesicles showed no changes in FRET over several hours (Fig. 1, E and F), as expected from the very low vesicle-vesicle exchange rates of phospholipids (12, 13).

The above results show that vesicles with high internal osmotic pressure can

acquire membrane from isotonic vesicles. These isotonic vesicles can lose membrane until they become spherical, but further membrane loss requires a volume decrease and concomitant concentration of their impermeable contents. The resulting osmotic gradient should eventually limit the redistribution of fatty acid. Indeed, as more swollen vesicles were added to a fixed number of initially isotonic vesicles, membrane loss reached a plateau (Fig. 2A). The maximum observed membrane loss from initially isotonic vesicles ($\sim 35\%$) was somewhat larger than the estimated membrane loss necessary to adopt a spherical shape ($\sim 27\%$; supporting online text), indicating that initially isotonic vesicles lost membrane until they also built up some osmotic gradient. Conversely, swollen vesicles, in the presence of excess isotonic vesicles, should grow until the membrane tension reaches zero, which we calculated should occur after a 35% surface area increase; the maximum observed increase was $\sim 35\%$.

To examine the mechanism of fatty acid transfer among vesicles, we tested the role of vesicle-vesicle collisions by varying the concentration of vesicles, but no rate changes were observed. Because the initial rate of uptake of fatty acid from micelles into vesicles can be quite fast compared with the observed rate of exchange (14), fatty acid adsorption is unlikely to be rate-limiting. We

also tested the role of fatty acid desorption from vesicles, which becomes faster as chain length decreases (15). Myristoleate vesicles (C14:1) showed faster exchange ($k_{\text{myristoleate}} \sim 0.6 \text{ s}^{-1}$). Exchange rates were also slower than fatty acid flip-flop rates (16). These observations indicate that exchange may be rate-limited by desorption, consistent with previous results on phospholipid transfer among liposomes (12, 17).

Having established that encapsulated osmolytes could drive vesicle growth at the expense of isotonic vesicles, we turned to vesicles that were osmotically swollen by encapsulated nucleic acids. Efforts to encapsulate high concentrations of nucleic acids ($>0.1 \text{ M}$ nucleotide monophosphate equivalents) in pure fatty acid vesicles caused visible aggregation and contents leakage. Because the addition of glycerol monoesters to fatty acid membranes has been reported to increase vesicle stability in the presence of high salt concentrations

Fig. 1. Stopped-flow mixing of isotonic and swollen oleate vesicles (1:1 molar ratio) in 0.2 M bicine, pH 8.5. Relative surface area was measured by the FRET assay; membrane growth decreases probe density, causing the FRET signal to decrease. Isotonic vesicles, labeled with FRET dyes, were mixed with unlabeled isotonic (A) or swollen (B) vesicles. The solid line indicates a single exponential decay curve fit with rate constant $k = 0.09 \text{ s}^{-1}$. Swollen vesicles, labeled with FRET dyes, were mixed with unlabeled swollen (C) or isotonic (D) vesicles. The solid line indicates the single exponential curve fit ($k = 0.08 \text{ s}^{-1}$). Isotonic (E) or swollen (F) POPC vesicles, labeled with FRET dyes, were mixed with unlabeled isotonic (open circles) or swollen (solid circles) POPC vesicles.

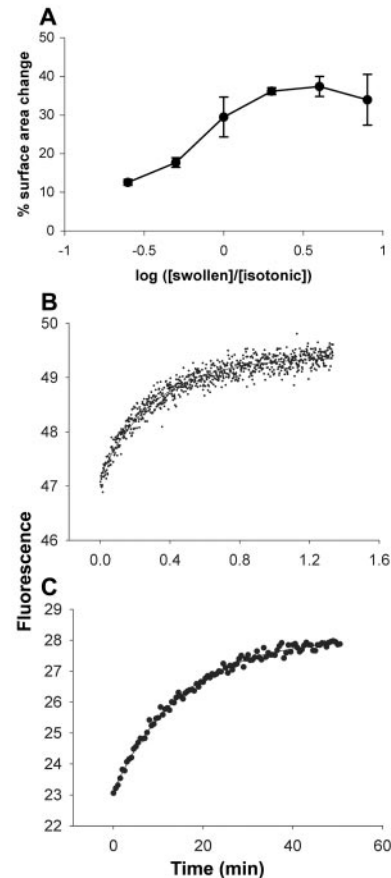
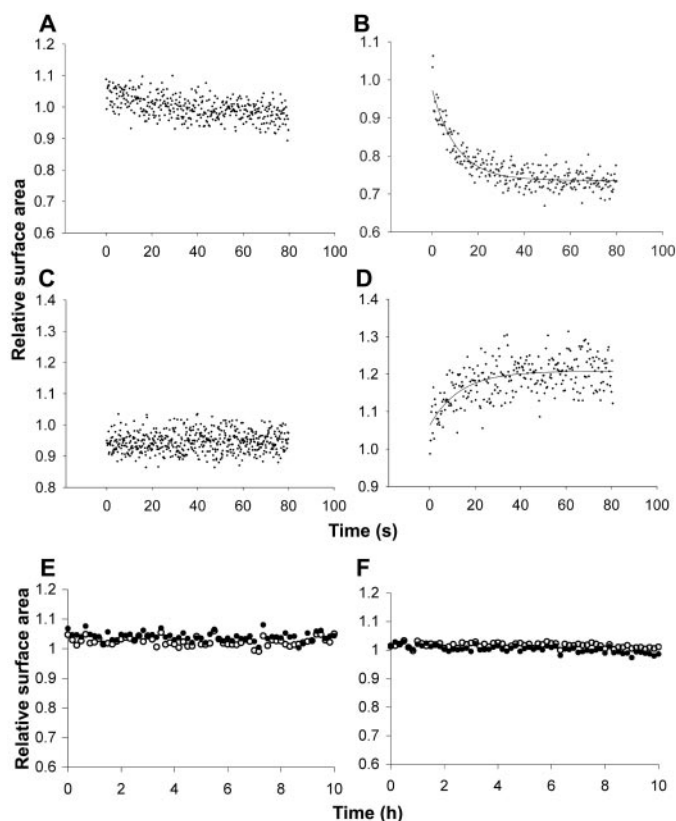


Fig. 2. (A) Change in surface area of isotonic vesicles mixed with different ratios of swollen vesicles, measured by FRET assay. Error bars indicate 95% confidence intervals for at least three trials. Time scale of intervesicular exchange of R18 in oleate (B) or MA:GMM (C) vesicles, measured by fluorescence dequenching. (B) Solid line indicates the single exponential curve fit ($k = 3.1 \text{ min}^{-1}$). (C) Solid line indicates a single exponential curve fit ($k = 0.06 \text{ min}^{-1}$).

(18), we encapsulated nucleic acids in myristoleate:glycerol monomyristoleate (MA:GMM = 2:1) vesicles, which were stable (supporting online text).

Initial competition experiments with MA:GMM vesicles were done using vesicles containing 0.2 M uridine 5'-monophosphate (5'-UMP) (~0.6 osmolar) (supporting online text). Growth of swollen vesicles and shrinkage of isotonic vesicles were observed as before (Table 1). The rate of exchange was substantially slower ($k_{MA:GMM} \sim 0.1 \text{ min}^{-1}$), consistent with the expected slower desorption rate from the more stable membranes. We confirmed that the difference between k_{oleate} and $k_{MA:GMM}$ quantitatively reflected the difference between the rate of lipid exchange in oleate versus that in MA:GMM vesicles using a self-quenching fluorescent fatty acid, octadecyl rhodamine B (R18) (6). Dilution of R18 among vesicles was detected as an increase in fluorescence (Fig. 2, B and C). The rate constant of R18 transfer in oleate vesicles (k^{R18}_{oleate}) was 3.0 min^{-1} , whereas $k^{R18}_{MA:GMM}$ was 0.06 min^{-1} (supporting online text). The fluorescence of R18-labeled vesicles did not change after mixing with buffer alone. These rate constants are in good agreement with the cor-

responding rate constants of osmotically driven lipid exchange.

Membrane transfer to swollen vesicles was also observed when the osmolyte was a heterogeneous mixture of RNA oligomers obtained by alkaline hydrolysis of bulk RNA (93 mg/ml; ~0.29 M nucleotide equivalents), which were 1 to 40 nucleotides in length as estimated by high-performance liquid chromatography. Finally, we observed membrane transfer using vesicles osmotically swollen by tRNA (83 mg/ml; ~0.26 M nucleotide equivalents), which has a length (72 to 95 bases) comparable to that of many ribozymes (19) (Fig. 3) (supporting online text).

The concentrations of nucleic acids that produce this effect are biologically reasonable. In general, the concentration of genomic nucleic acid in a unicellular organism increases as the size of the organism decreases. For one of the smallest bacteria, *Mycoplasma genitalium* (~300 nm in diameter), the concentration of DNA alone is 100 mg/ml (0.32 M nucleotide equivalents) (20). In a larger bacterium, *Escherichia coli*, the concentration of DNA is 13 mg/ml, and the combined concentration of DNA and RNA is ~130 mg/ml (0.4 M nucleotide equivalents) (21). The RNA concentrations used in our osmotically driven growth experiments fell within this range.

Our results show that osmotically swollen fatty acid vesicles can grow at the expense of relaxed (isotonic) vesicles. We have attempted to model the behavior of a primitive cell in which an RNA genome encodes functional RNA, but the same principles would apply given any other charged genetic polymer. In contrast, a neutral polymer such as PNA (peptide nucleic acid), having no associated counterions, would be a much less effective osmolyte, a difference that may have influenced the natural selection of the genetic material itself. We suggest that the phenomenon of osmotically driven, competitive vesicle growth could have played an important role in the emergence of Darwinian evolution

during the origin of cellular life (supporting online text). The present results suggest that simple physical principles may allow a direct connection between genome and membrane. RNA replicating within vesicles could confer a substantial growth advantage to the membrane by creating internal osmotic pressure. The faster replication of a superior replicase would therefore lead to faster vesicle growth, at the expense of cells lacking RNA or containing less efficient replicases. A faster replicase genotype would thus produce the higher-level phenotype of faster cellular growth, a prerequisite of cellular replication (supporting online text). Darwinian evolution at the organismal level might therefore have emerged earlier than previously thought—at the level of a one-gene cell.

Table 1. Intervesicle competition reactions using RNA osmolytes.

Osmolyte	FRET-labeled vesicles (low or high osmolarity)	% surface area change	k (min^{-1})
5'-UMP	Low	-45	0.05
	High	+36	0.02
Oligoribonucleotides*	Low	-64	0.03
	High	+51	0.02
tRNA	Low	-23	0.1
	High	+21	0.1

* Vesicles swollen by oligomers appeared to exchange more membrane than vesicles swollen by other osmolytes, an effect possibly due to salts or other minor components of bulk yeast RNA.

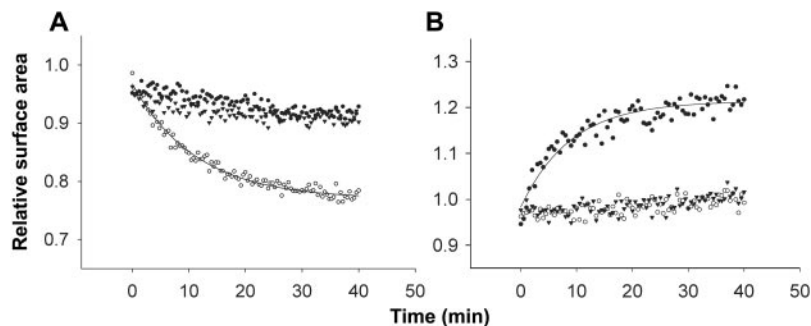


Fig. 3. Intervesicle competition using tRNA to swell MA:GMM vesicles. Isotonic (A) or swollen (B) vesicles were labeled with FRET dyes and mixed with unlabeled swollen vesicles pressurized by tRNA (open circles), isotonic vesicles (solid circles), or buffer only (triangles). (A) Solid line indicates a single exponential curve fit ($k = 0.09 \text{ min}^{-1}$). (B) Solid line indicates a single exponential curve fit ($k = 0.1 \text{ min}^{-1}$).

References and Notes

1. J. W. Szostak, D. P. Bartel, P. L. Luisi, *Nature* **409**, 387 (2001).
2. D. P. Bartel, P. J. Unrau, *Trends Cell Biol.* **9**, M9 (1999).
3. M. M. Hanczyc, S. M. Fujikawa, J. W. Szostak, *Science* **302**, 618 (2003).
4. J. M. Gebicki, M. Hicks, *Nature* **243**, 232 (1973).
5. P. Walde, R. Wick, M. Fresta, A. Mangone, P. L. Luisi, *J. Am. Chem. Soc.* **116**, 11649 (1994).
6. Materials and methods are available as supporting material on Science Online.
7. B. L. Mui, P. R. Cullis, E. A. Evans, T. D. Madden, *Biophys. J.* **64**, 443 (1993).
8. A. J. Jin, D. Huster, K. Gawrisch, R. Nossal, *Eur. Biophys. J.* **28**, 187 (1999).
9. S. D. Shoemaker, T. K. Vanderlick, *Ind. Eng. Chem. Res.* **41**, 324 (2002).
10. D. Needham, R. S. Nunn, *Biophys. J.* **58**, 997 (1990).
11. K. Olbrich, W. Rawicz, D. Needham, E. Evans, *Biophys. J.* **79**, 321 (2000).
12. L. R. McLean, M. C. Phillips, *Biochemistry* **20**, 2893 (1981).
13. J. D. Jones, T. E. Thompson, *Biochemistry* **28**, 129 (1989).
14. I. A. Chen, J. W. Szostak, *Biophys. J.* **87**, 988 (2004).
15. F. Zhang, F. Kamp, J. A. Hamilton, *Biochemistry* **35**, 16055 (1996).
16. I. A. Chen, J. W. Szostak, *Proc. Natl. Acad. Sci. U.S.A.* **101**, 7965 (2004).
17. J. E. Ferrell Jr., K. J. Lee, W. H. Huestis, *Biochemistry* **24**, 2857 (1985).
18. P. A. Monnard, C. L. Apel, A. Kanavarioti, D. W. Deamer, *Astrobiology* **2**, 139 (2002).
19. L. F. Landweber, P. J. Simon, T. A. Wagner, *Bioscience* **48**, 94 (1998).
20. H. J. Morowitz, *Beginnings of Cellular Life* (Yale Univ. Press, New Haven, CT, 1992).
21. J. D. Watson, *Molecular Biology of the Gene* (Benjamin, New York, ed. 1, 1965).
22. We are grateful to S. M. Fujikawa, M. M. Hanczyc, P.-A. Monnard, J. Carothers, and A. Luptak for helpful discussions. J.W.S. is an investigator of the Howard Hughes Medical Institute. I.A.C. was supported by the NIH Medical Scientist Training Program (T32-GM07753) and an NIH Molecular Biophysics Training Grant (T32-GM08313). This work was supported in part by a grant from the NASA Exobiology Program (EXB02-0031-0018).

Supporting Online Material

www.sciencemag.org/cgi/content/full/305/5689/1474/DC1
 Materials and Methods
 SOM Text
 References

26 May 2004; accepted 26 July 2004